



GEOSCIENCES

Thermal variations of the active layer in Fildes Peninsula, King George Island, Maritime Antarctica

ANDRÉ M. DE ANDRADE, ROBERTO F.M. MICHEL, ULISSES FRANZ BREMER, ELIAS DE LIMA NETO, GONÇALO BRITO T.G. VIEIRA, CARLOS ERNESTO G.R. SCHAEFER & JEFFERSON C. SIMÕES

Abstract: This work aimed to characterize the variation in the thermal regime of the active layer in a permafrost area on Fildes Peninsula, Antarctica, and relate this variability with meteorological data between 2014 and 2016. The monitoring site was installed to continuously monitor the temperature and moisture of the active layer, radiation flow on the surface, and air temperature. We used data collected to generate the indexes freezing degree-days, thawing degree-days, frost number, n-factor, apparent thermal diffusivity, and active layer thickness. The temperature of the active layer is not homogeneous, varying with depth and position in the transect, with the greatest variations in soil with better drainage and lower moisture content. Among the evaluated factors, air and soil surface temperature are the ones that most influence the thermal gradient of the active layer. We identified that near the surface there is a greater influence of albedo and cloudiness and at -35 cm depth there is a greater influence of net radiation and soil moisture. The average depth of the active layer in 2014 was -44.3 cm and in 2015 -47.7 cm and the frost number index indicates that there was a predominance of continuous permafrost in the transect during the monitoring.

Key words: active layer, maritime Antarctic, Permafrost, monitoring.

INTRODUCTION

In the second part of the 20th century, one of the highest warming rates on the planet was recorded in the Antarctic Peninsula, an increase of approximately 0.5 °C per decade (Turner et al. 2013), affecting the maritime Antarctic region (Turner et al. 2005). In Antarctica, regions located further north, such as the South Shetland Islands, are the most affected by the increase in air temperature (Skvarca & De Angelis 2003) changing the equilibrium of this fragile ecosystem.

Permafrost is a condition in which the soil remains frozen for at least two years (French 2007), it is estimated that 24% of the planet's exposed surfaces have experienced this condition (Slaymaker & Kelly 2007, Bockheim 2014). Permafrost is an essential component of the terrestrial cryosphere due to its carbon storage capacity (Cannone et al. 2006, Guglielmin et al. 2008) and fragility to climatic change (Kane et al. 2001).

The Antarctic permafrost, unlike the Arctic one, is not rich in carbon and its contribution to the emission of greenhouse gasses on a global scale is limited (Vieira et al. 2010). However, monitoring the active layer in areas with permafrost conditions is important for understanding the impacts of climate change in the Maritime Antarctic region (Romanovsky & Osterkamp 2000).

In this work, we aim to characterize the variation in the thermal regime of the active layer in a permafrost area on the Fildes Peninsula, Antarctica, and relate this variability with meteorological data between 2014 and 2016.

MATERIALS AND METHODS

Study Site

Fildes Peninsula is located in the southwestern region of King George Island in Maritime Antarctica (Figure 1). The peninsula covers 29.8 km² of ice-free area and has the largest ice-free surface on King George Island (Michel et al. 2014).

In Fildes peninsula, the oldest areas originated after the Collins Glacier retreat and periglacial geomorphological processes such as solifluction, cryoturbation and leveling prevail (Michel et al. 2014). The soil in ice-free areas has an incipient degree of development, especially when compared to other Antarctic locations, with a predominance of cryosols, often cryoturbed (Michel et al. 2014).

Fildes Peninsula has a polar maritime climate with strong winds, predominantly from the north, northwest and west (Vieira et al. 2014). The cold and humid climate has a mean annual air temperature of -2 °C, with a mean air temperature slightly above 0 °C during the summer and rarely below -12 °C in the winter (Wen et al. 1994). The annual rainfall varies between 350 mm and 500 mm, mainly in the summer (Øvstedal & Smith 2001).

Monitoring Site

The monitoring site was installed in January 2014, with maintenance and data collection activities taking place in 2015 and 2016. The monitoring site is located at 62°10,807 'S and 58°56,593' W at 111 m

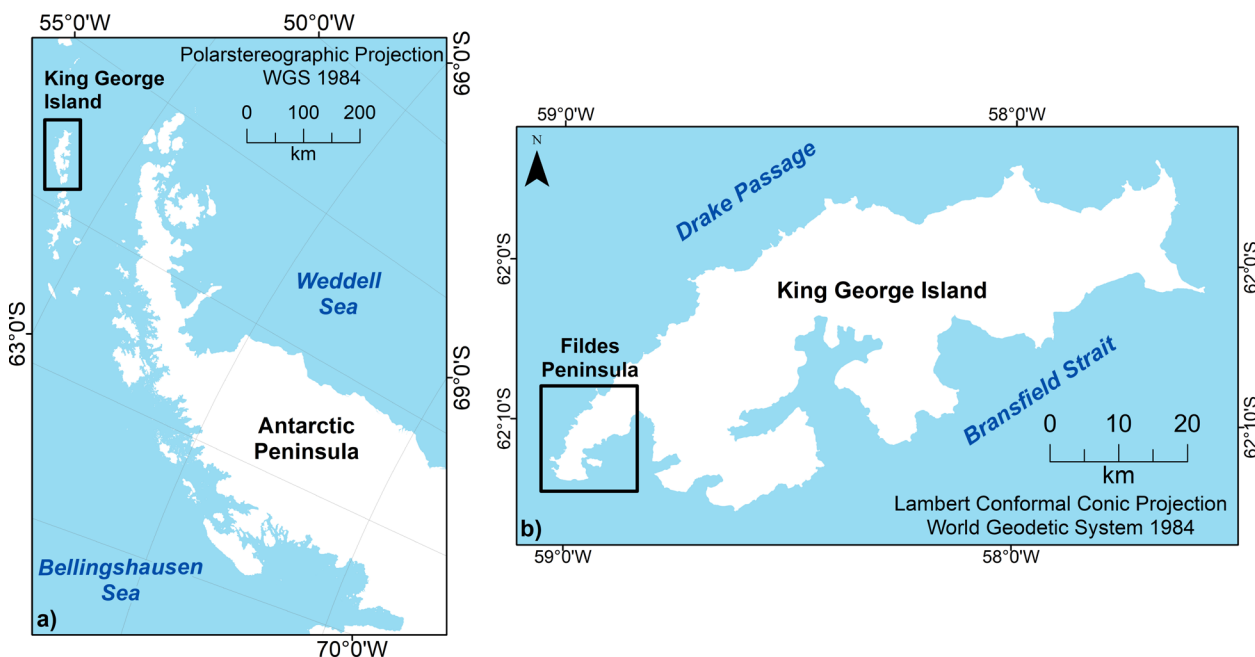


Figure 1. (a) Location of the Antarctic Peninsula, and (b) location of King George Island and highlight in Fildes Peninsula.

altitude and aims to continuously monitor the variability of temperature and moisture content of the active layer, short-wave and long-wave radiation flow on the surface, and air temperature.

In a 200 m long transect, 30 KT-20-L miniature temperature dataloggers with 0.5 °C precision were installed in 10 points with equidistance of 20 m. At each point temperature sensors were installed at depths of 5 cm, 20 cm and 35 cm, all capturing data independently at four-hour intervals.

To monitor the moisture of active layer we use a CS655 reflectometer at 35 cm deep to record the volumetric water content at hourly intervals. The energy flow on the surface was monitored using a CNR4 radiometer fixed at 1.80 m height about the surface to collect global radiation and reflected radiation, long wave radiation emitted by the atmosphere and the surface, air temperature, total radiation balance and the surface albedo between 0.305 μm and 2.8 μm and 4.5 μm to 42 μm . Figure 2 shows the location of the area where the monitoring site was installed in Meseta Norte on the Fildes Peninsula.

To broaden the analysis of meteorological variations, we use collected meteorological data between 1968 and 2015 by the Bellingshausen Station located on the Fildes Peninsula, 2.2 km from the monitoring site. The meteorological parameters that make up the time series data set used are shown in Table I.

Active Layer Thermal Regime

To understand the physical characteristics of the soil where the monitoring site is located, samples were collected in the soil profile for physical and chemical analysis. The determination of the textural pattern of the soil was done per slow mechanical dispersion in distilled water (pH 10), by sifting and weighing for the coarse and fine sand fractions, and by sedimentation for the silt and clay fractions. The mineralogical characterization of the sand, silt, and clay fractions was made from the collection of air-dried fine soil samples of the representative horizons of the three profiles.

Table I. Overview of meteorological parameters measured in this study. In the “Height/Depth” column, positive numbers refer to the height above the ground, while negative numbers refer to the depth.

Parameter	Instrument	Accuracy	Height/ Depth (cm)	Interval	Period
Net radiation	CNR4 Net Radiometer	Longwave radiation: $\pm 10\%$ Shortwave radiation: $\pm 4\%$	180	1 hour	2014-2016
Air temperature	107 Sensor	± 0.2 °C	100	1 hour	2014-2016
Ground surface temperature	KT-20-L	± 0.5 °C	- 5, -20, -35	4 hours	2014-2016
Soil moisture	CS655	$\pm 3\%$	-35	1 hour	2014-2016
Insolation	Bellingshausen station	-	-	Monthly	1986-2016
Cloud cover	Bellingshausen station	-	-	Monthly	1986-2016
Precipitation	Bellingshausen station	-	-	Monthly	1986-2016
Atmospheric pressure	Bellingshausen station	-	-	Monthly	1986-2016
Air temperature	Bellingshausen station	-	-	Monthly	1986-2016
Ground surface temperature	Bellingshausen station	-	-	Monthly	1986-2016
Relative humidity	Bellingshausen station	-	-	Monthly	1986-2016
Wind components	Bellingshausen station	-	-	Monthly	1986-2016

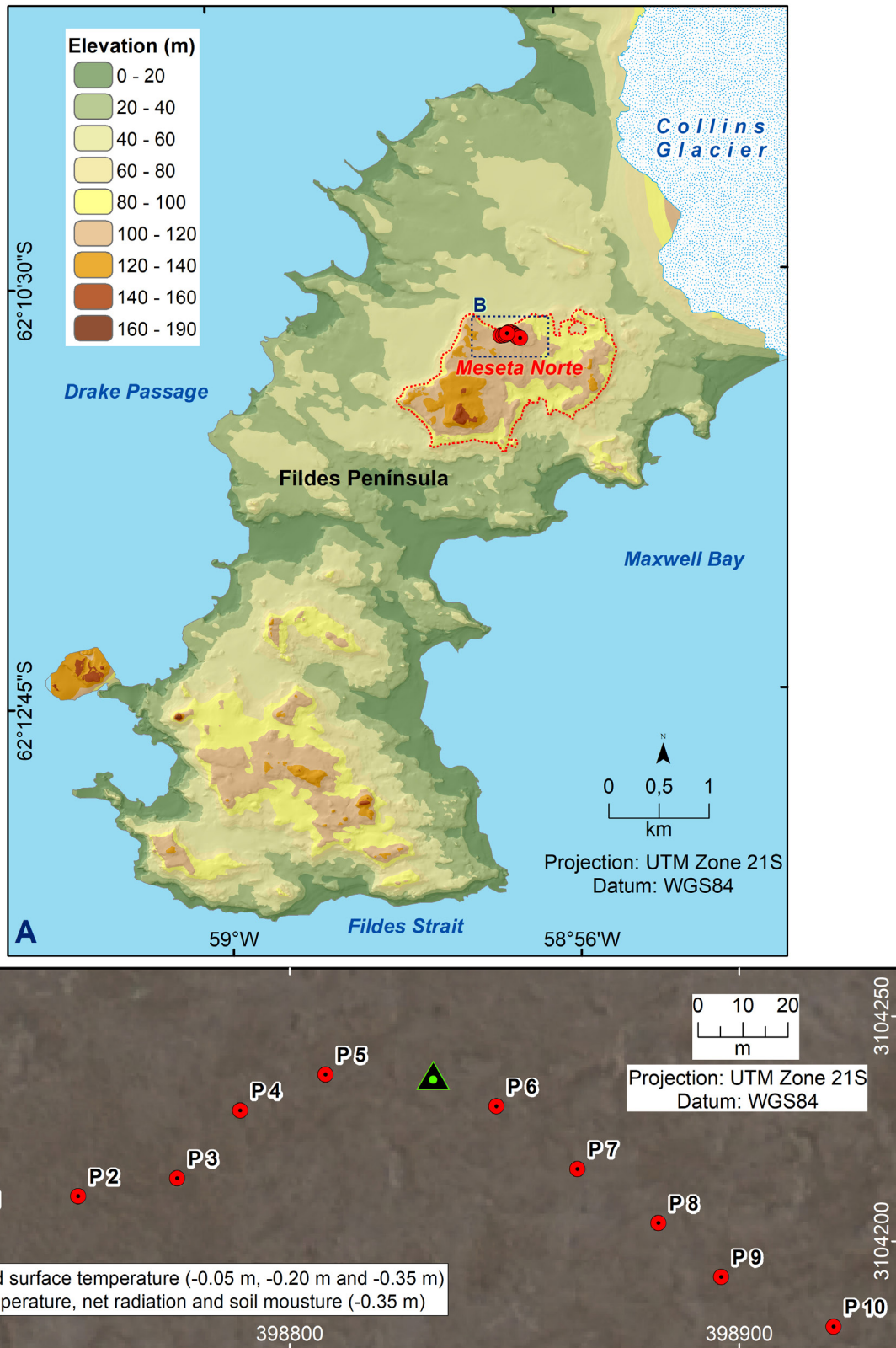


Figure 2. (a) digital elevation model and highlight for Meseta Norte in Fildes peninsula; (b) location of the monitoring site, including a Quickbird image as a background.

To assess the energy balance and magnitudes of thawing and freezing of the active layer, the daily averages were considered according to the freezing degree-days (FDD) and thawing degree-days (TDD) indexes (Guglielmin et al. 2008). The TDD was estimated through the cumulative sum of the average daily temperatures above 0 °C of the entire data series and the FDD from the cumulative sum of the average daily temperatures below 0 °C.

The thermal variation of the active layer is seasonal (Bockheim & Hall 2002, Vieira et al. 2010, Michel et al. 2014) and the analysis of daily variations was made using the methodology proposed by Guglielmin et al. 2008, where the temperature data series of the active layer was classified daily according to the prevailing thermal conditions at each depth in the different points of the transect. The classification uses four classes defined by Guglielmin et al. 2008: thawed days (all active layer temperatures are positive and at least one was above 0.5 °C), frozen days (all active layer temperatures are negative and at least one is below -0.5 °C), isothermal days (all temperatures varied between ±0.5 °C), and freeze-thaw days (there are variations in negative and positive temperatures, with at least one value above or below ±0.5 °C).

The Frost Number (FN) index was used to detect locations with the occurrence of permafrost through calculations that consider the degree of freezing and thawing of the soil (Nelson & Outcalt 1987). The FN values indicate the limits of the regions that present the condition for continuous permafrost (FN ≥ 0.67), discontinuous permafrost (0.67 > FN ≥ 0.6), sporadic permafrost (0.6 > FN ≥ 0.5), and absence of permafrost (FN < 0.5). The FN index was obtained using equation 1:

$$FN = \frac{FDD^{0.5}}{FDD^{0.5} + TDD^{0.5}} \tag{1}$$

where *FDD* is freezing degree-days (air °C day), *TDD* is thawing degree-days (air °C day), and *FN* is frost number ranging between 0 and 1.

The N-factor (Nf) was estimated by the ratio between the sum of the FDD of the soil temperature and the surface air temperature, with values close to 1 indicating a small difference between the degree days products of the soil temperatures and air. Values below 1 indicating that the air temperature is higher than the temperature in the ground (Klene et al. 2001). The Nf estimate was made using equation 2:

$$Nf = \frac{FDD_s}{FDD_a} \tag{2}$$

where *FDD_s* are the freezing degree-days for ground surface temperature and *FDD_a* means freezing degree-days for air temperature.

Table II. Soil physical characteristics along the transect in February 2016.

Site	Depth (cm)	Soil moisture (%)	Organic matter	Coarse sand	Fine sand	Silt	Clay	Texture classes
P1	-10	9.48	2.79	63.0	9.3	15.2	12.4	Sandy-loam
P1	-20	13.13	2.15	35.7	18.7	31.7	13.9	Sandy-loam
P5	-10	12.57	3.17	53.4	22.3	13.3	11.0	Sandy-loam
P5	-20	13.29	2.91	42.8	17.7	30.0	9.5	Sandy-loam
P10	-10	5.78	1.01	68.6	8.3	13.8	9.3	Sandy-loam
P10	-20	12.53	2.03	48.8	17.2	22.7	11.3	Sandy-loam

The influence of the surface energy balance in the variations of the active layer was estimated through the heat fluxes in the inner portion of the soil using apparent thermal diffusivity (ATD) for Tundra soils (McGaw & Outcalt 1978) and adapted by Michel et al. 2014:

$$ATD = \left(\frac{\Delta Z^2}{2 \Delta t} \right) \times \left(\frac{[T_i^{j+1} - T_i^{j-1}]}{[T_j^{i-1} - 2T_j^i + T_j^{i+1}]} \right) \quad (3)$$

where ATD is the apparent thermal diffusivity (m^2s^{-1}), ΔZ : spatial increment (m), Δt : temporal increment (s), T: internal temperature ($^{\circ}\text{C}$), j: temporal position, and i: depth. This procedure assesses the energy flow in the profile, and the estimates were made for each hour in the intermediate depths of the profiles, and the average values were calculated for each day of the time series.

The active layer thickness (ALT) was estimated using the deepest temperature measurements in the profile considering the maximum thickness reached by the 0°C isotherm at the end of the thawing season (Guglielmin 2006). To define the depth with a thermal gradient of 0°C , we used a linear interpolation of the temperature with a depth of 35 cm.

The monitored meteorological parameters were analyzed using stepwise multivariate regression to assess and rank the influence on the variation of the active layer. The stepwise method was applied through the sequential introduction of variables combining the forward and backward methods (Chong & Jun 2005) through the sequential insertion of the variable with the highest bivariate correlation with the temperature of the active layer. Through this method, a model was developed with the smallest number among the 18 statistically significant independent variables and with maximum precision to explain the dependent variable.

RESULTS AND DISCUSSION

Due to cryoturbation processes, the chemical and physical characteristics of the soil in the transect have a predominance of sandy loam texture (Table II). The sand fraction is predominant in the three points, corresponding to 67.2% of the particles smaller than 2 mm, while the content of the fine fraction, silt, and clay correspond to 21.1% and 11.2% respectively. The physical characteristics of the soil in the study site were similar to those found elsewhere in Maritime Antarctica (Michel et al. 2006, 2014, Almeida et al. 2014).

The soil profile showed less volumetric water content when close to the surface increasing in the depth, both the coarse texture of the profile and high evapotranspiration contribute to this distribution. The low development of the profile and its limited depth together with the permafrost table create a drainage impediment at the bottom of the active layer generating temporary hydromorphic conditions in summer.

The greatest difference in soil moisture occurred close to the surface, with 6.79% between P1 and P10, while at 35 cm there was less contrast, with a maximum difference of 0.76% between P5 and P10. Despite the slight variation in moisture content at the points, in P10 the soil had more efficient drainage, while in P5 there was higher moisture content near the surface and deeper.

Soil texture influences water retention, drainage and thermal gradient in the soil profile. The profiles presented a sandy loam texture, with the largest composition of sand fraction (coarse and fine) in P10, comprising 71%, while P5 and P1 showed 68.1% and 63.4% respectively. The sand fraction,

Table III. Mean monthly air and soil temperature and soil moisture between 2014 and 2016. The ground temperature was obtained through the mean of the points in each depth on the transect.

Year	Month	Temperature (°C)				Soil moisture (%)
		Air	Ground surface (cm)			Depth (cm)
			-5	-20	-35	-35
2014	2	-0.50	0.95	0.73	0.61	12.60
	3	-1.38	-0.17	0.23	0.30	11.26
	4	-1.86	-1.28	-0.78	-0.44	12.60
	5	-3.66	-2.23	-1.38	-0.93	7.95
	6	-5.03	-4.26	-3.72	-3.28	6.98
	7	-3.93	-3.27	-3.13	-2.97	7.02
	8	-6.22	-4.41	-4.11	-3.85	6.90
	9	-4.94	-3.53	-3.60	-3.56	6.90
	10	-3.29	-1.46	-1.90	-2.10	7.09
	11	-3.00	-0.41	-0.91	-1.12	7.32
	12	-0.96	1.40	0.22	-0.02	8.01
	2015	1	0.11	2.58	1.50	0.74
2		0.38	2.47	1.96	1.19	18.81
3		-0.34	1.17	0.53	0.35	18.38
4		-1.20	-0.35	-0.28	-0.04	13.06
5		-4.21	-2.56	-1.78	-1.05	6.63
6		-8.40	-7.28	-6.71	-5.49	4.01
7		-6.63	-7.75	-7.42	-6.52	3.95
8		-7.46	-5.90	-5.87	-5.55	4.01
9		-7.01	-6.60	-6.55	-6.12	3.97
10		-3.78	-1.82	-2.61	-2.79	4.27
11		-1.61	-0.37	-1.27	-1.37	4.60
12		-0.86	2.05	0.43	-0.13	4.62
2016	1	-1.44	2.97	2.25	0.79	4.63
	2	-1.40	2.38	1.91	1.16	4.65
Mean		-3.15	-1.51	-1.69	-1.69	8.71
Minimum		-8.40	-7.75	-7.42	-6.52	3.95
Maximum		0.38	2.97	2.25	1.19	18.81
Standard deviation		2.56	3.23	2.84	2.41	4.50

due to its reduced water retention capacity and abundance of macropores, provides better soil drainage, while the silt and clay fractions have high microporosity and contribute to greater water retention, reducing soil drainage.

The average annual air temperature at Fildes Peninsula in 2014 and 2015 was $-2.92\text{ }^{\circ}\text{C}$ and $-3.44\text{ }^{\circ}\text{C}$ respectively, while the highest average daily temperature occurred on 01/31/2015 ($3.06\text{ }^{\circ}\text{C}$) and the lowest $-16.24\text{ }^{\circ}\text{C}$ on 08/16/2015. The average air temperature in the summer of 2014 and 2015 was $-0.45\text{ }^{\circ}\text{C}$ and $0.14\text{ }^{\circ}\text{C}$, indicating a variation of $0.59\text{ }^{\circ}\text{C}$ in the period. The average temperature in the winter of 2014 was $-4.89\text{ }^{\circ}\text{C}$ and $-7.82\text{ }^{\circ}\text{C}$ in 2015. Considering the data series between 1968 and 2015, the average air temperature in the summer was $1.10\text{ }^{\circ}\text{C}$ and $-5.70\text{ }^{\circ}\text{C}$ in winter, signifying that the

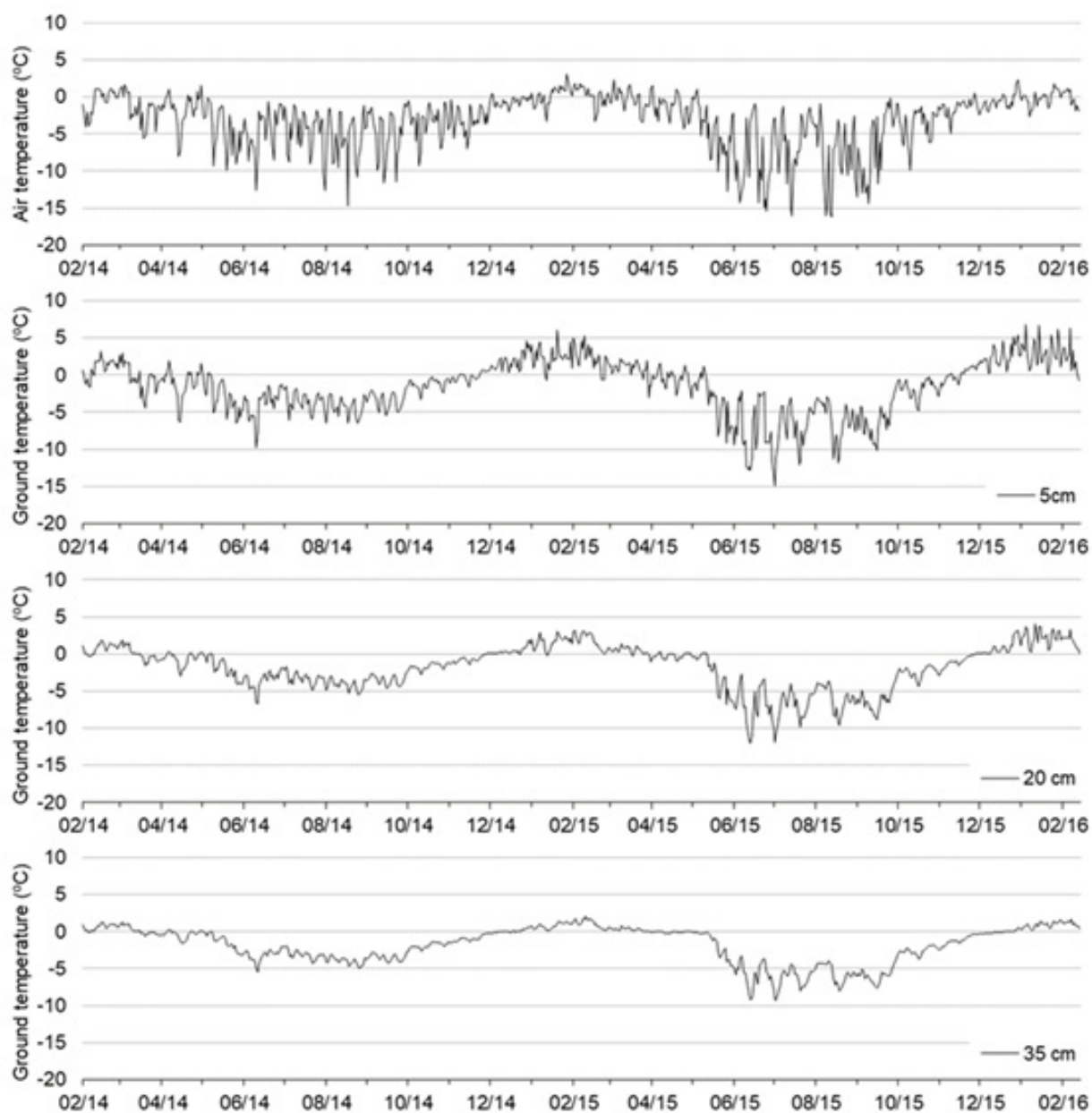


Figure 3. Daily average of air temperature and active layer temperature in the transect at depths of 5 cm, 20 cm, and 35 cm in Fildes peninsula between February 2014 and February 2016.

average temperatures of both seasons of 2014 and 2015 were lower than the historic average (Figure 3 and Table III).

The active layer temperature showed seasonal variations according to depth and location, indicating that the thermal variation of the active layer is influenced by factors in different ways. At 5 cm depth, the maximum temperature of 7.50 °C was recorded on P9 on 01/24/2015 and the minimum of -19.08 °C on P6 on 07/05/2015. At 35 cm, the maximum temperature of 5.67 °C also occurred at P9 but on 01/11/2015 while the minimum temperature of -12.50 °C was recorded at P10 on 07/05/2015 (Figure 3 and Table III).

The average potential solar activity on Fildes peninsula in winter was 7h 41min day⁻¹ and 16h 27min day⁻¹ in summer. These values represent the estimate of the duration of the insolation if there were no meteorological interference in solar activity.

The freezing of the active layer starts with temperatures below 0 °C. During the monitored period, the freezing of the active layer started in the superficial layer and, through the loss of latent heat in the vertical gradient of the profile, gradual freezing advanced to greater depths.

In 2014, the freezing of the active layer started at 5 cm homogeneously in the transect between May 11th and 13th, while the freezing at the depth of 20 cm started at P2 and P6 on May 13th. The time difference between the beginning of freezing at 5 cm and at 35 cm varied in the two years monitored, with the longest interval being 10 days, with the beginning of freezing at both depths on the same day in some points. The occurrence in some points of the simultaneous onset of freezing in both 5 cm and 35 cm occurred due to the double freezing front with the influence of the superficial conditions in the depth of 5 cm and the permafrost in the greatest depths.

In 2015 the beginning of the freezing of the active layer also occurred in May. In P8, at a depth of 35 cm, the freezing started on the 19th, while in other points, the beginning occurred later than in 2014. The largest interval between the difference between the beginning of freezing in 5 cm and 35 cm was seven days in P6. In the remaining points, the average interval was three days.

Thawing in 2014 started at the 5 cm layer at all points in late November, except for P2, which started thawing 16 days in advance. In 2015, the 5 cm thaw started between November 19th on P9 and January 19th on P8. In that year, the thaw at 35 cm depth began on January 8, 16 days earlier compared to 2014.

The average interval between the start of thawing at depths of 5 cm and 35 cm in 2014 was 14 days. The thawing of the active layer in the two years of monitoring started in November at a depth of 5 cm. In 2015, the interval between the start of thawing in the profile was greater in P2 with 56 days. In other points, the average interval was 24 days.

The average temperature of the active layer in the transect registered seasonal variations in the two years analyzed (Figure 4). The temperature in summer increased continuously, while in winter there were two strong temperature reductions. This behavior is influenced by the zero-curtain effect that buffers temperature variations in the water phase change, slowing the freezing process of the active layer.

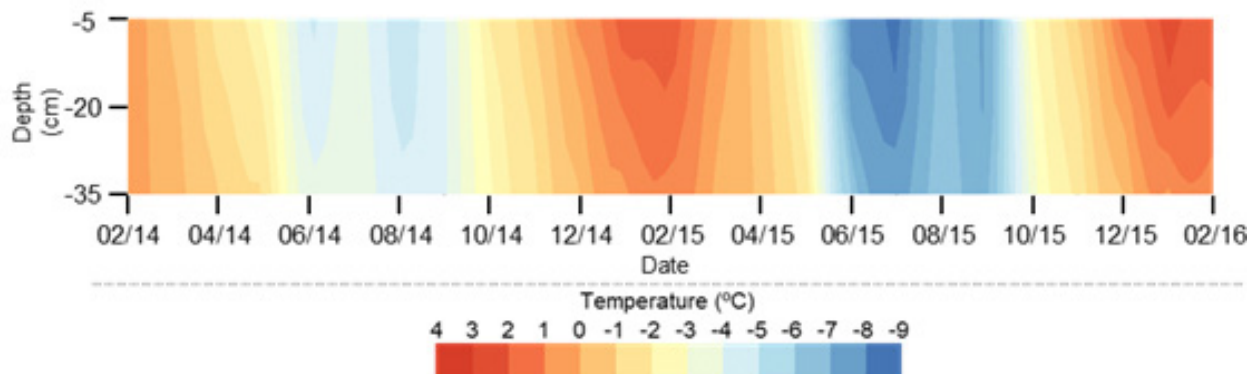


Figure 4. Thermogram plotted from the active layers average temperature registered in the transect in Meseta Norte, Fildes Peninsula, between 2014 and 2016.

The onset of freezing in the transect was similar to that found in another monitoring site at Fildes Peninsula located near the Escudero Station on a slope oriented towards Maxwell Bay (Michel et al. 2014). At other monitoring sites located on King George Island, the onset of freezing of the active layer occurred earlier than recorded in this study. The freeze on the Keller Peninsula started in March (Chaves et al. 2017) and at the end of March in Lions Rump (Almeida et al. 2014) and Low Head (Almeida et al. 2016).

The start of thawing of the active layer in the transect showed a pattern of similarity with the beginning of thawing in other monitoring sites on King George Island (Almeida et al. 2014, Michel et al. 2014). The beginning of thawing in the Keller Peninsula was similar only with some points of the transect and at 35 cm of depth (Chaves et al. 2017).

The 35 cm soil moisture measured showed high amplitude (Table III). The period with the highest moisture content in the soil was between January and April with 14.7%, while the lowest average soil moisture was between June and October with 5.5%. The reduction of the moisture content in the soil starts concomitantly with the freezing period of the active layer, strongly influenced by the freezing or thawing of the active layer, the melting of surface snow, and rainfall.

Despite the proximity, the characteristics of the environment in the transect differ and therefore differences are expected in the measured data. The area where points T1 to T5 are installed is characterized by temporary hydromorphism due to the shallow Cryosol. At the other end where the T8 to T10 sensors are located, the surface is slightly higher (≈ 1 m to 2 m), resulting in soils with better drainage and less moisture content. In general, the AB horizon of the soil in this study area is frequently affected by cryoturbation processes (Michel et al. 2014).

The estimated ALT is not uniform in the transect, in 2014 there were variations between -39 cm and -55 cm, and in 2015 from -40 cm to -65 cm. The average increase in ALT in 2015 may reflect the reduction in average air temperature in winter between 2014 and 2015. During this period, the most significant increase in ALT occurred in P10 from -47 cm to -65 cm and the most significant reduction was in P9 from -55 cm to -46 cm. The variation in ALT recorded between P1 and P5 was lower than that between P6 and P10 due to the higher moisture content that contributes to reducing sudden variations in temperature (Figure 5).

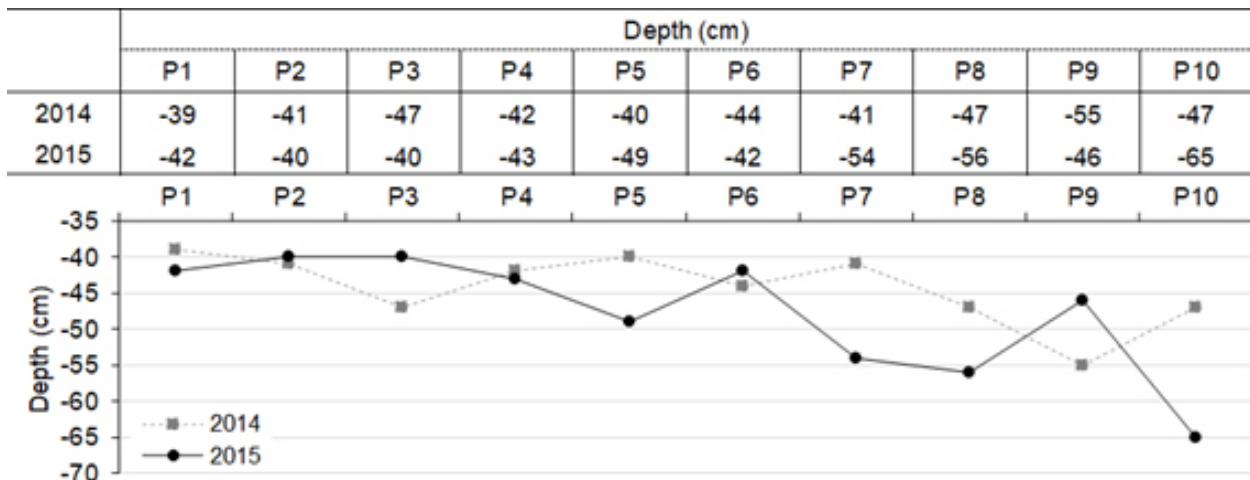


Figure 5. Active layer thickness estimated in the transect in 2014 and 2015.

The ALT estimated in this study (111 m a.s.l.) ranged from -39 cm to -65 cm, with an average depth in 2014 of -44.3 cm and -47.7 cm in 2015. ALT in the Meseta Norte transect is shallower than those estimated in most of the monitoring sites on King George Island. ALT in another location on the Fildes Peninsula (65 m a.s.l.) ranged from -89 cm to -106 cm (Michel et al. 2014), in Lions Rump (85 m a.s.l.) ranged from -120 cm to -147 cm (Almeida et al. 2014) and in Low Head (94 m a.s.l.) it varied between -98 cm to -106 cm (Almeida et al. 2016). In Keller Peninsula (90 m a.s.l.) the ALT varied between -64 cm and -75 cm (Chaves et al. 2017), therefore having ALT similar to the maximum value measured in this study. In Deception Island (130 m a.s.l.), which had its formation originating from volcanoclastic sediments, ALT varied from -46 cm to -67 cm (Goyanes et al. 2014). On James Ross Island (41 m a.s.l.), which has a colder and less humid climate, ALT varied between -52 cm and -64 cm (Hrbáček et al. 2017). The ALT registered in the Keller Peninsula, Deception Island, and James Ross Island has values similar to those recorded in this study.

The temperature at the three depths of the active layer in the two years of monitoring had 58.6% of freezing days, 22.4% of thawing days, followed by freeze-thaw days and isothermal days with 10% and 9%, respectively (Figure 6).

At 5 cm depth there were 54.5% freezing days, 23.1% freeze-thaw days, 21.1% thawing days, and only 1.3% isothermal days. The freezing days occur mainly between May and October, while the thawing days occur between December and March, mainly in February. The months of November and April exhibit characteristics of transition between freezing and thawing days. In the period there were few isothermal days, with the highest concentration in April with 26 isothermal days. The thaw-freeze days occurred between December and April without a predominant phase.

The thermal variability at a depth of 35 cm exhibits 60% of freezing days, while thawing days comprise 22%, isothermal days 15.4%, and freezing-thawing days 2.6%. The increase in isothermal days at 35 cm is related to the zero-curtain effect when at the beginning of the period of freezing and thawing at greater depths the temperature remains constant due to the latent heat flow dispersed during the changes in the water phase.

The TDD and FDD indexes showed spatial and temporal variation. In the three depths, the highest temperatures occurred in January and February and the lowest temperatures between June and August. We found 66% of the sum of TDD in 5 cm occurred in January (1661 °C day) and February (984 °C day), at 35 cm the predominance of monthly TDD inverted, with 682 °C in February and 480 °C in January. The maximum TDD in the vertical gradient of the soil occurred during the summer, having subsequently reduced during the fall. In winter, TDD did not exist and increases again in the spring (Figure 7).

The thermal variation of FDD is opposite to that of TDD, with the highest values concentrated between late autumn and early spring (Figure 8). At 5 cm the maximum FDD occurred in June with -2588 °C day. At 35 cm, the months of July, August, and September present -2900 °C day, equivalent to about 60% of the total FDD.

The sum of TDD and FDD grouped by depth indicates the occurrence of 49% and 32% respectively at a depth of 5 cm, indicating that the thawing process has a greater impact when close to the surface due to the influence of local surface and meteorological conditions. The freezing of the soil is more intense 35 cm due to the freezing in two fronts; however, it presents a more homogeneous distribution along the three depths of the active layer, indicating that this process occurs due to the loss of energy in the soil.

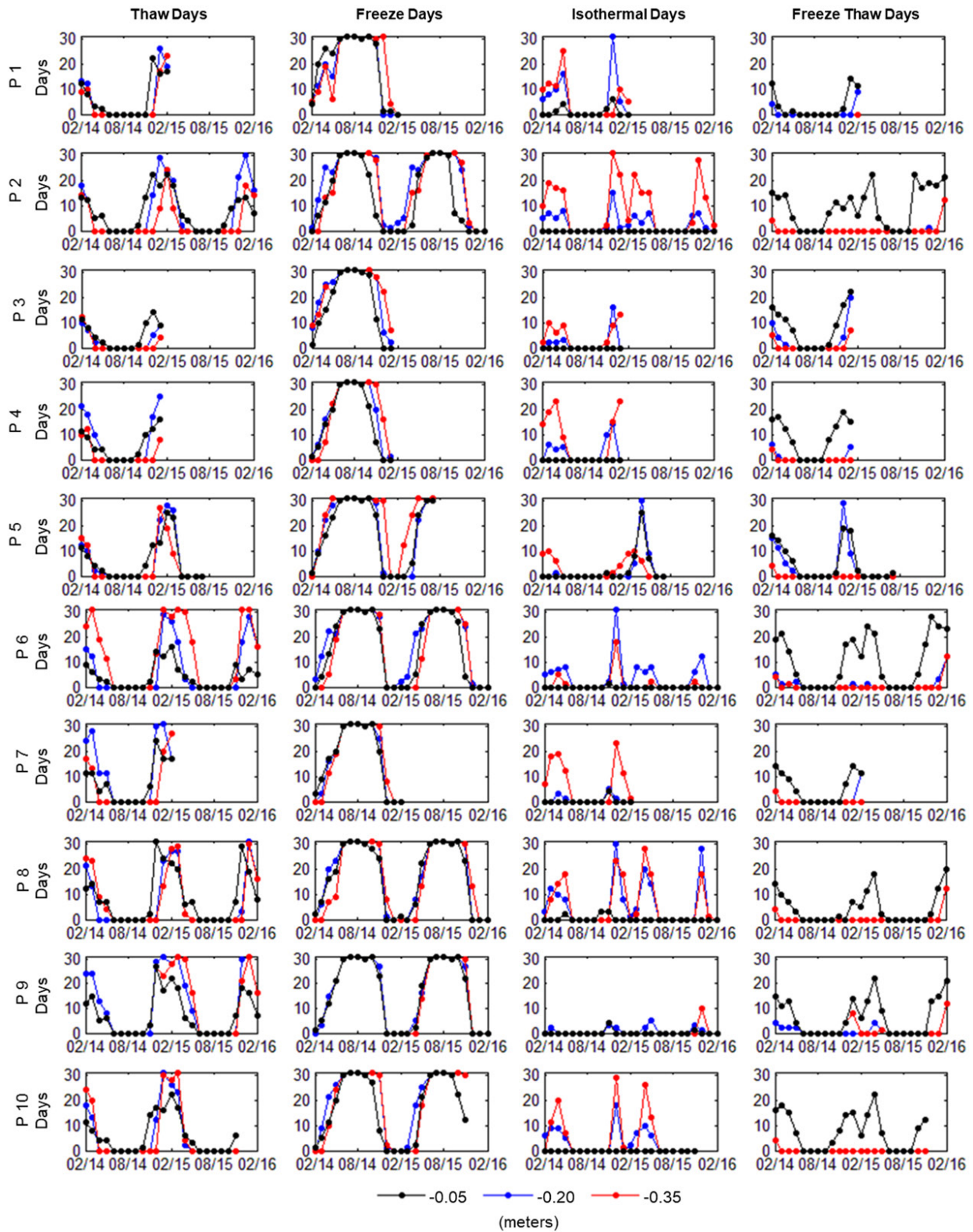


Figure 6. Thaw days, freeze days, isothermal days, and freeze-thaw days along the transect from 2014 to 2016.

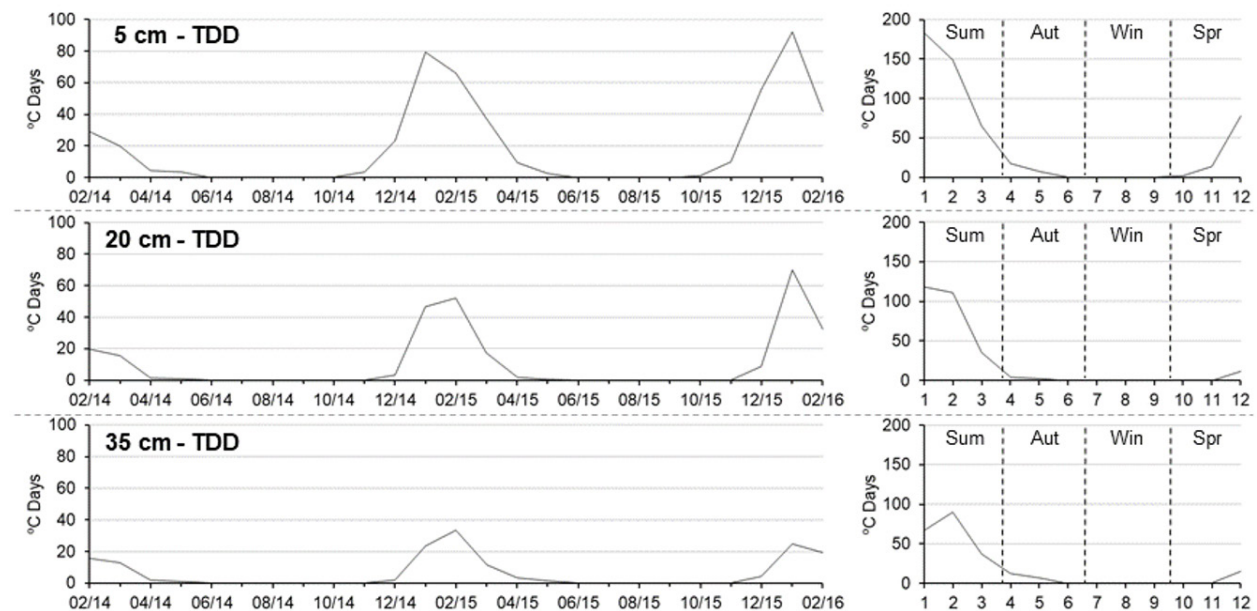


Figure 7. Average thawing degree-days -TDD (°C Days) in the transect at depths 5 cm, 20 cm, and 35 cm between February 2014 to February 2016 and cumulative monthly average of TDD by season.

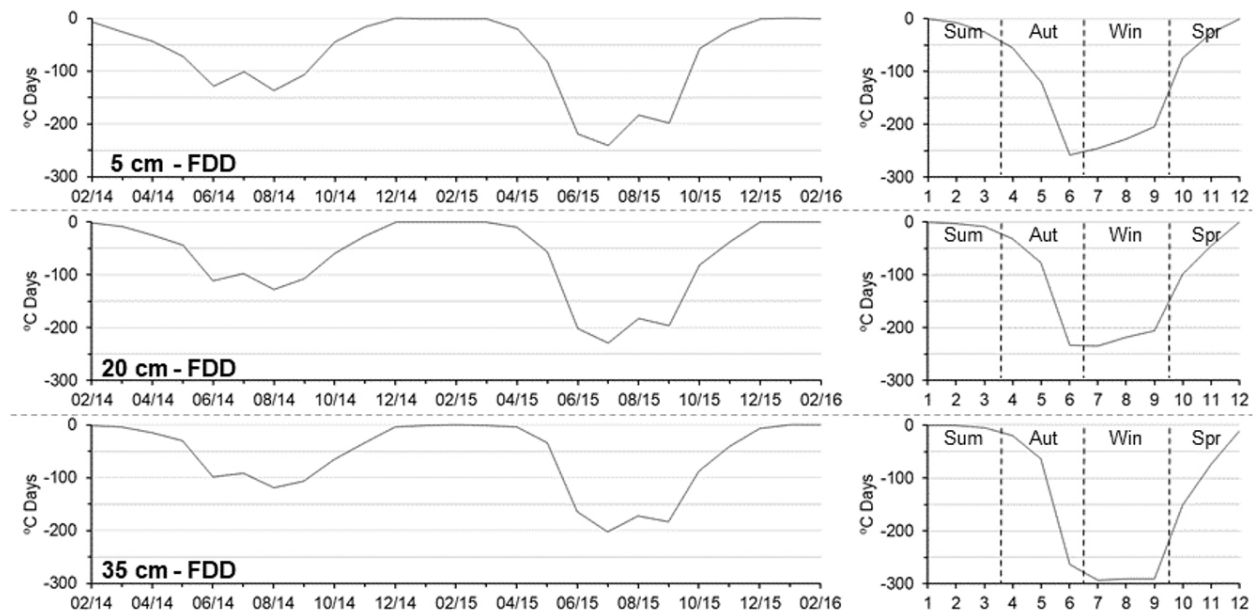


Figure 8. Average freezing degree-days – FDD (°C Days) in the transect at depths 5 cm, 20 cm and 35 cm between February 2014 to February 2016 and cumulative monthly average of FDD by season.

The ATD in the active layer is also influenced by seasonal variations during the thawing and freezing conditions of the soil (Hinkel 1997). At both ends of the transect, the lowest ATD values occurred in winter and autumn, while in the center of the transect, the lowest values occurred in winter and spring (Table IV). The highest average ATD occurred in the summer of 2016, and the lowest average ATD occurred in the fall. The values point to the higher thermal conductivity of the soil in seasons with higher temperatures in response to the incidence of energy and soil moisture conditions.

The behavior of thermal diffusivity estimated in this study is similar to the values obtained at other monitoring sites in Maritime Antarctica (De Pablo et al. 2013, Michel et al. 2014, Almeida et al. 2016).

The FN index indicates that in 2014 all points had a condition of continuous permafrost with values of the highest indices of 0.76 and 0.73 in P6 and P8 respectively. In 2015, P6 and P8 maintained a condition of continuous permafrost with FN 0.68 and 0.67 respectively, while P2 and P9 with an FN of 0.63 showed discontinuous permafrost. In both years there was a reduction in FN at all points in the transect, even though the average air temperature in 2015 was lower than in 2014, indicating that other local factors also influence the energy flow.

The lowest values of the Nf occurred between January and March, the period with the highest air temperatures. After the reduction in air temperatures, the Nf values gradually decreased until reaching the lowest values in December. During the monitoring period in the transect the highest mean Nf was 0.58 in P6 and in the other points the highest values were approximately 0.45. The maximum Nf value in P6 may be due to the condition of higher soil moisture in that location (Figure 9).

Table IV. Summary of apparent thermal diffusivity (ATD) average in -0.20 m depth along the transect in the seasons.

Season	Average ATD in -0.20 m ($\times 10^4 \text{ m}^2\text{s}^{-1}$)									
	P1	P2	P3	P4	P5	P6	P7	P8	P9	P10
Summer-14	0.87	114.45	92.41	16.78	68.19	12.61	-6.49	0.93	0.17	9.14
Autumn-14	-27.66	30.74	25.33	8.83	-60.23	19.58	-12.87	16.25	9.18	-8.68
Winter-14	0.07	0.51	0.39	0.68	0.19	0.05	0.12	0.08	-0.03	0.28
Spring-14	-14.13	39.35	14.55	6.00	-64.56	0.51	-11.95	-7.04	-9.45	2.75
Summer-15	39.34	78.76	N	N	-74.79	0.01	-6.40	-20.68	27.03	39.28
Autumn-15	N	39.64	N	N	-0.43	0.00	N	-65.38	1.22	2.78
Winter-15	N	0.67	N	N	0.10	0.00	N	0.10	0.19	0.56
Spring-15	N	46.44	N	N	N	0.00	N	5.18	-9.54	-2.15
Summer-16*	N	178.37	N	N	N	0.02	N	-33.60	121.61	N
Average	N	58.77	N	N	N	0.02	N	-11.57	15.60	5.49
Standard deviation	N	54.01	N	N	N	0.02	N	23.49	38.87	13.60

*Data registration until 02/17/2016; N: data record failure.

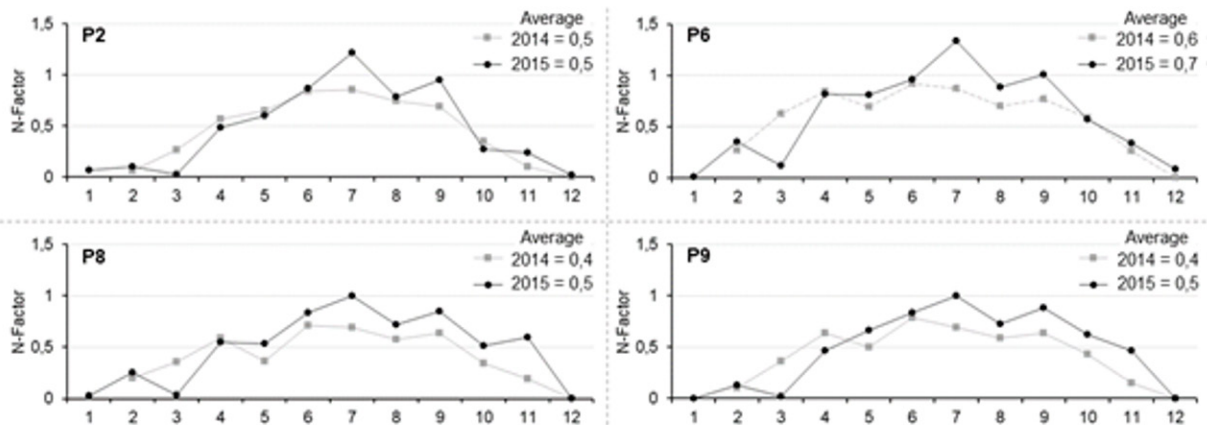


Figure 9. Changes in average n-factors over four monitoring points in the years 2014 and 2015. We use the temperature at -5 cm which is close to the ground surface.

The portion of the transect located between P6 and P10 showed the greatest variability in the soil temperature during monitoring. This pattern is confirmed by noting that the minimum temperatures in 5 cm and 35 cm occurred in P6 and P10 respectively and the maximum temperatures in 5 cm and 35 cm occurred in P9. ALT had the largest variations in P10 and the highest TDD values in 35 cm occurred in P9. The highest FDD values in 35 cm occurred in P3, the lowest ATD was in P8, and the highest Nf in P6.

Thermal changes in the active layer and relationship with meteorological conditions

The thermal variation of the active layer is influenced by local meteorological conditions and is a variable that depends on the meteorological variables used in this study to generate the multiple regression model (Figure 10). The selection of independent variables to compose the regression model was based on the values obtained in the estimate of Pearson’s correlation (r) between external variables and variables related to the temperature of the active layer at the three depths (Table V). External variables with $r > 0.4$ were selected as potential variables for inclusion in the model.

In 5 cm deep, the variable with the highest bivariate correlation was air temperature ($r = 0.951$), which was used to create the first linear regression with a variable. The analysis of variance obtained $R^2 = 0.905$ and a reduction of 90.5% of the error, which was statistically significant (Table VI). In the following steps, other individual variables were included in the model and the determination of the variables maintained or discarded in the equation was done with a significance level of 0.05, 167 degrees of freedom (g.l.), and a critical value of 1.980. The f value of the variable air temperature was

Table V. Pearson correlation coefficient of variables used in stepwise regression models at depths of -0.05 m and -0.35 m.

Variables	Ground surface temperature	
	-5 cm	-35 cm
Albedo (%)	0.437*	0.227*
Insolation (hours)	0.679*	0.517*
Cloud cover (tenths)	0.418*	0.367*
Precipitation (mm)	0.111	0.182*
Atmospheric pressure (hPa)	-0.212	0.046
Upward longwave radiation (Wm^{-2})	0.315*	0.387*
Downward longwave radiation (Wm^{-2})	0.239*	0.313*
Shortwave net radiation (Wm^{-2})	0.706*	0.660*
Longwave net radiation (Wm^{-2})	-0.201*	-0.168*
Global radiation (Wm^{-2})	0.516*	0.346*
Net radiation (Wm^{-2})	0.638*	0.599*
Reflected Shortwave (Wm^{-2})	0.121	-0.023
Air temperature (°C)	0.951*	0.916*
Ground surface temperature (°C)	0.945*	0.913*
Relative humidity (%)	-0.054	0.220*
Soil moisture (-0.35 m)	0.769*	0.774*
Wind direction (°)	0.135	-0.007
Wind speed (ms^{-1})	-0.323*	-0.288*

* $P < 0.05$.

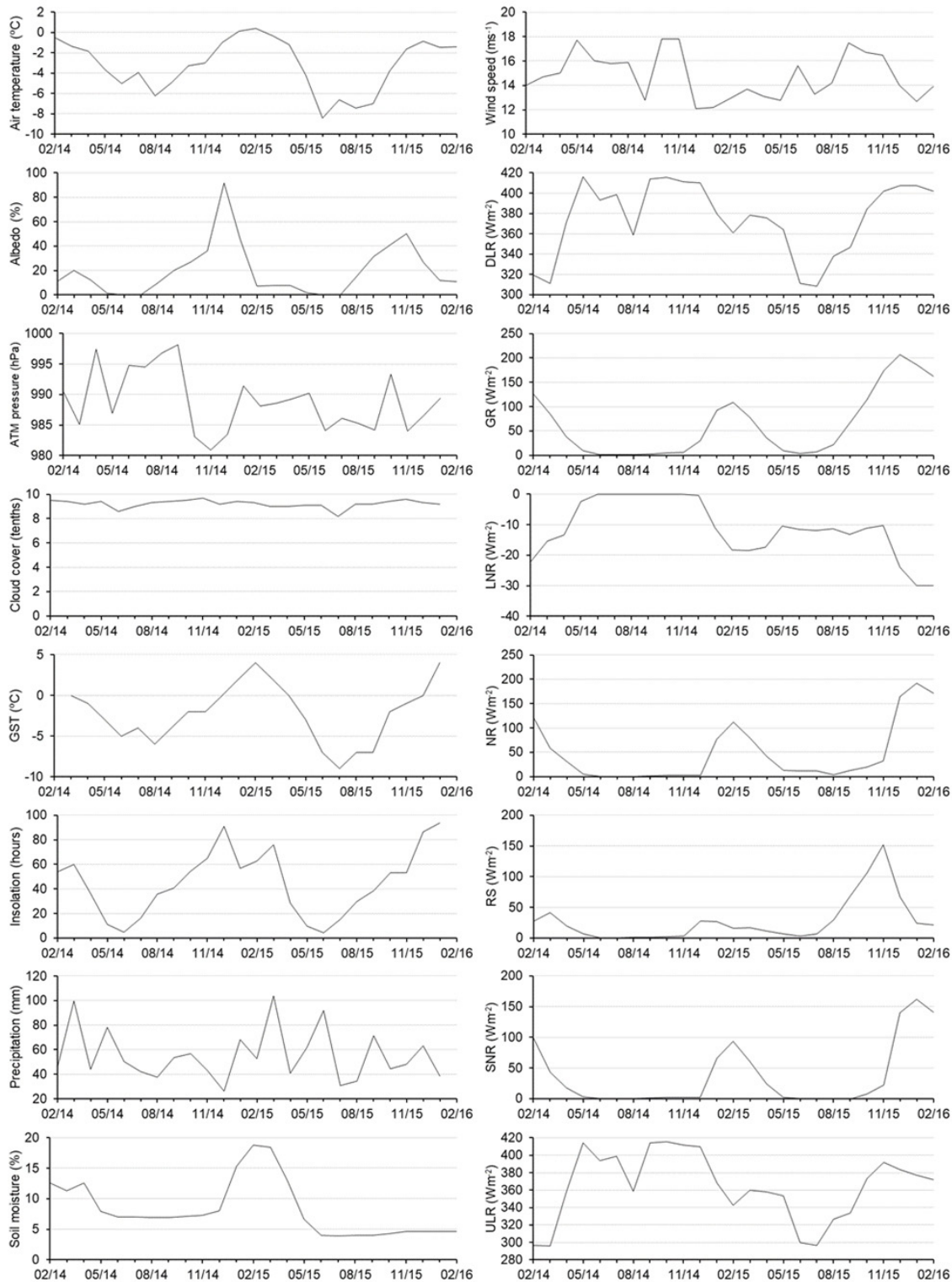


Figure 10. Monthly average Meteorological data from Fildes peninsula between 2014 and 2016 analyzed with thermal changes of the active layer. ATM pressure: atmospheric pressure, GST: Ground Surface Temperature, DLR: Downward longwave radiation, GR: Global radiation, LNR: Longwave net radiation, NR: Net radiation, RS: Reflected shortwave, SNR: Shortwave net radiation, ULR: Upward longwave radiation.

adequate for the reference and, because it is statistically significant, it was inserted as a predictor variable of the temperature variation of the active layer in 5 cm.

The second variable added to the model was the ground surface temperature ($r = 0.945$) resulting in an increase in R^2 to 0.915 and a reduction in the standard error of the estimate from 0.4 to 0.379, indicating that there was an improvement in the general adjustment of the model. The difference in the regression coefficients for the two variables was due to multicollinearity ($r = 0.966$). The third variable inserted in the model was albedo, increasing R^2 to 0.921. The cloudiness presented the same R^2 as the albedo, however, the albedo was chosen due to its higher variation coefficient (0.412 and 0.478 respectively). The highest coefficient indicates a slight predominance of the albedo with the temperature variation of the active layer at that depth. The fourth and last variable included in the 5 cm regression model was cloudiness, but it resulted in a slight increase of 0.3% to the general R^2 .

The external variable with the highest correlation in 35 cm was also air temperature ($r = 0.916$), indicating that this is the external variable with the greatest contribution to the thermal gradient in the active layer. However, there was a reduction in the influence of this variable at greater depths, denoting that in greater depths there are other variables that influence the thermal behavior of the active layer. The regression model with air temperature results in $R^2 = 0.838$.

The second variable inserted into the regression model at a 35 cm depth was the ground surface temperature ($r = 0.913$ and $R^2 = 0.851$). The third variable inserted was net radiation ($r = 0.599$ and $R^2 = 0.864$) and the fourth and last variable inserted was soil moisture ($r = 0.774$ and $R^2 = 0.882$) (Table VII).

The regression model that best suits the thermal variability in 35 cm differs from that obtained for 5 cm. The temperature at the soil surface is influenced by the air temperature, and the correlation

Table VI. Explaining variables in the multiple regression for ground surface temperature in -5 cm.

Dependent variable Ground surface temperature -5 cm	Explaining variables			
	1	2	3	4
	Air temp.	Air temp. GST	Air temp. GST Albedo	Air temp. GST Albedo Cloud cover
R^2	0.905	0.915	0.921	0.924
Adjusted R^2	0.904	0.914	0.920	0.922
Standard error	0.400	0.379	0.366	0.360
Significance F	0.000	0.000	0.000	0.000

Air temp.: air temperature; GST: ground surface temperature.

Table VII. Explaining variables in the multiple regression for ground surface temperature in -35 cm.

Dependent variable Ground surface temperature -35 cm	Explaining variables			
	1	2	3	4
	Air temp.	Air temp. GST	Air temp. GST Net radiation	Air temp. GST Net radiation Soil moisture
R^2	0.838	0.851	0.864	0.882
Adjusted R^2	0.836	0.850	0.862	0.880
Standard error	0.445	0.428	0.410	0.383
Significance F	0.000	0.000	0.000	0.000

Air temp.: air temperature; GST: ground surface temperature.

between these two variables is 0.966. The increase in air temperature and the earth surface confirm the conduction of energy within the soil profile. The differences in the models occurred in the third and fourth variables at both depths. While at 5 cm there is a strong influence of Albedo and cloud cover, at 35 cm, the variables with strong influence are net radiation and Soil Moisture.

The albedo varied mainly when the surface was covered with snow, and in periods without snow cover, there was a predominance of albedo characteristic of dark rocks. Seasonal variations in snow cover directly interfere with the absorption of solar radiation by surface components (Choi et al. 2008) and influence the thermal regime of the active layer (Ling & Zhang 2003).

The high cloudiness and the few days of clear skies in Fildes Peninsula (Vieira et al. 2014) limit the incidence of solar radiation. In this way, cloudiness also influences the thermal variability of the active layer close to the surface. The net radiation and the soil moisture interfere with the variability of the active layer mainly at 35 cm of depth. The net radiation resulting from the short-wave and long-wave radiation flow with great influence on soil freezing (Li et al. 2014) and on the melting of surface snow (Ling & Zhang 2003). Net radiation also interferes with ablation, especially in periods with a negative balance of long-wave radiation, which can contribute to 64% of ablation (-2017754214 Bintanja 1995). The variability of the radiation balance depends not only on the fluctuation in the incidence of solar radiation but also on changes in the characteristics of the superficial albedo (-2017754214 Bintanja 1995) and the balance of long-wave radiation (Li et al. 2014).

The soil moisture had a greater influence on the thermal variability of the active layer in 35 cm. The moisture content interferes with the energy transmission capacity in the soil profile and facilitates the energy flow mainly via percolation (Michel et al. 2014). It also interferes with the heat exchange during the alteration of the freezing and thawing phases (Guglielmin et al. 2008, Almeida et al. 2014) and in the spatial variability of ALT (Hrbáček et al. 2017), being important in the regulation of the transmission capacity of energy in the vertical gradient of the soil, considering that water absorbs and releases energy during the phases of change of its physical state.

The relationship between the thermal variability of the active layer and the meteorological and environmental variables has also been evaluated elsewhere in Antarctica. At Arctowski Station located in Admiralty Bay, the air temperature and global radiation exhibited a strong and moderate correlation with the temperature of the active layer in the portions closest to the surface and a weak correlation at 70 cm depth (Araźny et al. 2013). Similar results were obtained using multivariate regression, noting that the air temperature has a strong correlation with the temperature variation in the active layer at Lions Rump (Almeida et al. 2014) and in the Ross Sea region (Adlam et al. 2010)

The equations of the regression models obtained for 5 cm and 35 cm depths are presented in equations 4 and 5. These equations show the effects exerted by the set of independent variables on the temperature variability of the active layer in the transect. The models obtained explain 92.4% and 88.2% of the thermal variability of the active layer in 5 cm and 35 cm depth respectively.

$$y_{5cm} = -2,345 + 0,336 x_{air\ temperature} + 0,116 x_{GST} + 0,316 x_{albedo} + 0,303 x_{cloud\ cover} \quad (4)$$

$$y_{35cm} = -0,273 + 0,159 x_{air\ temperature} + 0,186 x_{GST} - 0,012 x_{net\ radiation} + 7,485 x_{soil\ moisture} \quad (5)$$

CONCLUSIONS

Active layer monitoring in this work shows slight differences in thermal variability when compared to other studies on King George Island. The maximum thawing of the active layer was during ablation and coincided with periods with higher air temperatures and in the other periods, the freezing condition predominated. The thermal variability in the transect is not homogeneous, varying according to position and depth, a condition verified by the amplitude in thickness of the active layer in the transect, which varied between -39 cm and -65 cm between 2014 and 2016. Among the factors evaluated, air temperature and ground surface temperature are the ones that most influence the thermal variation of the active layer. We identified other factors that influence the thermal variation of the active layer, at 5 cm depth the albedo and cloud cover, while at 35 cm depth the net radiation and soil moisture. Other meteorological factors also influence the thermal variability of the active layer, but they do not show statistical significance. Precipitation also impacts the environment due to higher temperatures than snow and ice on the surface. However, due to the low precision of the precipitation data acquired in this region of Antarctica, it had no statistically significant values when added to the model.

Acknowledgments

This study was supported by Coordenação de Aperfeiçoamento de Pessoal de Nível Superior (CAPES), Conselho Nacional de Pesquisas e Instituto Nacional de Ciência e Tecnologia da Criosfera CNPq/INCT 465680/2014-3, Brazilian National Institute of Cryospheric Science and Technology, Proantar, Brazilian Navy, Federal University of Rio Grande do Sul (UFRGS) and Federal University of Viçosa (UFV)

REFERENCES

- ADLAM LS, BALKS MR, SEYBOLD CA & CAMPBELL DI. 2010. Temporal and spatial variation in active layer depth in the McMurdo Sound Region, Antarctica. *Antarct Sci* 22: 45-52.
- ALMEIDA ICC, SCHAEFER CEGR, FERNANDES RBA, PEREIRA TTC, NIEUWENDAM A & PEREIRA AB. 2014. Active layer thermal regime at different vegetation covers at Lions Rump, King George Island, Maritime Antarctica. *Geomorphology* 225: 36-46.
- ALMEIDA ICC, SCHAEFER CEGR, MICHEL RFM, FERNANDES RBA, PEREIRA TTC, ANDRADE AM, FRANCELINO MR, FERNANDES-FILHO EI & BOCKHEIM JG. 2016. Long term active layer monitoring at a warm-based glacier front from maritime Antarctica. *Catena* 149: 572-581.
- ARAŻNY A, KEJNA M & SOBOTA I. 2013. Ground temperature at the Henryk Arctowski Station (King George Island, Antarctic) – case study from the period January 2012 to February 2013. *Bull Geogr* 6: 59-80.
- BINTANJA R. 1995. The local surface energy balance of the Ecology Glacier, King George Island, Antarctica: measurements and modelling. *Antarct Sci* 7: 315-325.
- BOCKHEIM JG. 2014. *Cryopedology*, New York: Springer, 173 p.
- BOCKHEIM JG & HALL KJ. 2002. Permafrost, active-layer dynamics and periglacial environments of continental Antarctica. *S Afr J Sci* 98: 82-90.
- CANNONE N, ELLIS-EVANS JC, STRACHAN R & GUGLIELMIN M. 2006. Interactions between climate, vegetation and the active layer in soils at two Maritime Antarctic site. *Antarctic Science*. Cambridge University Press 18: 323-333.
- CHAVES DA, LYRA GB, FRANCELINO MR, SILVA LDB, THOMAZINI A & SCHAEFER CEGR. 2017. Active layer and permafrost thermal regime in a patterned ground soil in Maritime Antarctica, and relationship with climate variability models. *Sci Total Environ* 15: 572-585.
- CHOI T, LEE BY, KIM SJ, YOON YJ & LEE HC. 2008. Net radiation and turbulent energy exchanges over a non-glaciated coastal area on King George Island during four summer seasons. *Antarct Sci* 20: 99-111.
- CHONG IG & JUN CH. 2005. Performance of some variable selection methods when multicollinearity is present. *Chemometrics and Intelligent Laboratory Systems* 78: 103-112.
- DE PABLO MA, BLANCO JJ, MOLINA A, RAMOS M, QUESADA A & VIEIRA G. 2013. Interannual active layer variability at

the Limnopolar Lake CALM site on Byers Peninsula, Livingston Island, Antarctica. *Antarct Sci* 25: 167-180.

FRENCH HM. 2007. *The Periglacial Environment*, 3rd ed., Ottawa: J Wiley & Sons Ltd., 480 p.

GOYANES G. ET AL. 2014. Régimen térmico y variabilidad espacial de la capa activa en isla Decepción, Antártida. *Rev Asoc Geol Argent* 71: 112-124.

GUGLIELMIN M. 2006. Ground surface temperature (GST), active layer, and permafrost monitoring in continental Antarctica. *Permafrost Periglacial Process* 17: 133-143.

GUGLIELMIN M, ELLIS-EVANS CJ & CANNONE N. 2008. Active layer thermal regime under different vegetation conditions in permafrost areas. A case study at Signy Island (Maritime Antarctica). *Geoderma* 144: 73-85.

HINKEL KM. 1997. Estimating seasonal values of thermal diffusivity in thawed and frozen soils using temperature time series. *Cold Reg Sci Technol* 26: 1-15.

HRBÁČEK F, NÝVLT D & LÁSKA K. 2017. Active layer thermal dynamics at two lithologically different sites on James Ross Island, Eastern Antarctic Peninsula. *Catena* 149: 592-602.

KANE DL, HINKEL KM, GOERING DJ, HINZMAN LD & OUTCALT SI. 2001. Non-conductive heat transfer associated with frozen soils. *Global Planet Change* 29: 275-292.

KLENE AE, NELSON FE & SHIKLOMANOV NI. 2001. The N-factor in Natural Landscapes: Variability of Air and Soil-Surface Temperatures, Kuparuk River Basin, Alaska, U.S.A. *Arct Antarct Alp Res* 33: 140-148.

LI R. ET AL. 2014. The impact of surface energy exchange on the thawing process of active layer over the northern Qinghai-Xizang Plateau, China *Environ Sci* 72: 2091-2099.

LING F & ZHANG T. 2003. Impact of the Timing and Duration of Seasonal Snow Cover on the Active Layer and Permafrost in the Alaskan Arctic. *Permafrost Periglacial Process* 14: 141-150.

MCGAW RW & OUTCALT SI. 1978. Thermal Properties and Regime of Wet Tundra Soils at Barrow, Alaska. In: *Third International Conference on Permafrost*. National Research Council of Canada. Ottawa: Canada. 47-53.

MICHEL RFM, SCHAEFER CEGR, LÓPEZ-MARTÍNEZ J, SIMAS FNB, HAUS NW, SERRANO E & BOCKHEIM JG. 2006. Soils and landforms from Fildes Peninsula and Ardley Island, Maritime Antarctica. *Geomorphology* 225: 76-86.

MICHEL RFM, SCHAEFER CEGR, MARTÍNEZ JL, SIMAS FNB, HAUS NW, SERRANO E & BOCKHEIM JG. 2014. Soils and landforms from Fildes Peninsula and Ardley Island, Maritime Antarctica. *Geomorphology* 225: 76-86.

NELSON FE & OUTCALT SI. 1987. A computational method for prediction and regionalization of permafrost. *Arct Antarct Alp Res* 19: 279-288.

ØVSTEDAL DO & SMITH RIL. 2001. *Lichens of Antarctica and South Georgia: A guide to their Identification and Ecology*, Cambridge: Cambridge University Press, 453 p.

ROMANOVSKY VE & OSTERKAMP TE. 2000. Effects of unfrozen water on heat and mass transport processes in the active layer and permafrost. *Permafrost Periglacial Process* 11: 219-239.

SKVARCA P & DE ANGELIS H. 2003. Impact assessment of regional climatic warming on glaciers and ice shelves of the northeastern Antarctic Peninsula. *Antarctic Peninsula Climate Variability* 79: 69-78.

SLAYMAKER O & KELLY REJ. 2007. *The Cryosphere and Global Environmental Change*, Blackwell Publishing, 305 p.

TURNER J ET AL. 2013. Antarctic climate change and the environment: an update. *Polar Rec* 50: 1-23.

TURNER J, COLWELL SR, MARSHALL GJ, LACHLAN-COPE TA, CARLETON AM, JONES PD, LAGUN V, REID PA & IAGOVKINA S. 2005. Antarctic climate change during the last 50 years. *Int J Climatol* 25: 279-294.

VIEIRA G ET AL. 2010. Thermal State of Permafrost and Active-layer Monitoring in the Antarctic: Advances During the International Polar Year 2007-2009. *Permafrost Periglacial Process* 21: 182-197.

VIEIRA G, MORA C, PINA P & SCHAEFER CER. 2014. A proxy for snow cover and winter ground surface cooling: Mapping *Usnea* sp. communities using high resolution remote sensing imagery (Maritime Antarctica). *Geomorphology* 225: 69-75.

WEN J, KANG J, XIE Z, HAN J & ALBERT L. 1994. Climate, mass balance and glacial changes on small dome of Collins Ice Cap, King George Island, Antarctica. *Antarct Res* 5: 52-61.

How to cite

ANDRADE TM, MICHEL RFM, BREMER UF, DE LIMA NETO E, VIEIRA GBTG, SCHAEFER CEGR & SIMÕES JC. 2023. Thermal variations of the active layer in Fildes Peninsula, King George Island, Maritime Antarctica. *An Acad Bras Cienc* 95: e20230181. DOI 10.1590/0001-3765202320230181.

*Manuscript received on February 24, 2023;
accepted for publication on November 6, 2023*

ANDRÉ M. DE ANDRADE¹

<https://orcid.org/0000-0003-3502-7847>

ROBERTO F.M. MICHEL²

<https://orcid.org/0000-0001-5951-4610>

ULISSES FRANZ BREMER³

<https://orcid.org/0000-0003-0519-5807>

ELIAS DE LIMA NETO⁴

<https://orcid.org/0000-0002-5985-9245>

GONÇALO BRITO T.G. VIEIRA⁵

<https://orcid.org/0000-0001-7611-3464>

CARLOS ERNESTO G.R. SCHAEFER⁶

<https://orcid.org/0000-0001-7060-1598>

JEFFERSON C. SIMÕES³

<https://orcid.org/0000-0001-5555-3401>

¹Universidade Federal dos Vales do Jequitinhonha e Mucuri, Avenida Universitária, 1000, 38620-870 Unaí, MG, Brazil

²Universidade Estadual de Santa Cruz, Rodovia Jorge Amado, Km 16, 45662-900 Ilhéus, BA, Brazil

³Universidade Federal do Rio Grande do Sul, Avenida Bento Gonçalves, 9500, 91501-970 Porto Alegre, RS, Brazil

⁴Universidade de São Paulo, Avenida Trabalhador São-carlense, 400, 13566-590 São Carlos, SP, Brazil

⁵Universidade de Lisboa, Rua Branca Edmée Marques, 1600-276, Lisboa, Portugal

⁶Universidade Federal de Viçosa, Avenida Peter Henry Rolfs, s/n, 36570-900 Viçosa, MG, Brazil

Correspondence to: **André Medeiros de Andrade**

E-mail: andre.medeiros@ufvjm.edu.br

Author contributions

Performed field work and conceptualization: André Andrade, Roberto Michel, Elias Neto, Gonçalo Vieira and Ulisses Bremer. Data analysis and wrote the paper: André Andrade, Roberto Michel and Ulisses Bremer. Funding acquisition: Carlos Schaefer, Jefferson Simões and Ulisses Bremer.

